



Title	Sulfide-Induced Dimerization Versus Demetallation of Tricopper(I) Clusters Protected by Tris-Thiolato Metalloligands
Author(s)	Goo, Zi Lang; Yoshinari, Nobuto; Yasukawa, Yuhei et al.
Citation	Chemistry - An Asian Journal. 2024, 19(13), p. e202400266
Version Type	VoR
URL	https://hdl.handle.net/11094/97146
rights	This article is licensed under a Creative Commons Attribution 4.0 International License.
Note	

The University of Osaka Institutional Knowledge Archive : OUKA

<https://ir.library.osaka-u.ac.jp/>

The University of Osaka

Sulfide-Induced Dimerization Versus Demetallation of Tricopper(I) Clusters Protected by Tris-Thiolato Metalloligands

Zi Lang Goo,^[a, b] Nobuto Yoshinari,^{*[a]} Yuhei Yasukawa,^[a] Katsue Minami,^[a] and Takumi Konno^{*[a, c]}

Here, we report the reactivity of copper(I) clusters toward sulfide ions; these sulfide copper(I) clusters have attracted much attention due to their relevance to biologically active centers and their fascinating structural and photophysical properties. Treatment of the $\text{Cu}_3\text{Rh}^{\text{III}}_2$ pentanuclear complex, $[\text{Cu}_3\{\text{Rh}(\text{aet})_3\}_2]^{3+}$ (aet = 2-aminoethanethiolate), in which a $\{\text{Cu}^{\text{I}}_3\}^{3+}$ cluster moiety is bound by two *fac*- $[\text{Rh}(\text{aet})_3]$ metalloligands, with NaSH in water produced the $\text{Cu}_6\text{Rh}^{\text{III}}_4$ decanuclear complex, $[\text{Cu}_6\text{S}\{\text{Rh}(\text{aet})_3\}_4]^{4+}$, accompanied by the dimeri-

zation of $[\text{Cu}_3\{\text{Rh}(\text{aet})_3\}_2]^{3+}$ and the incorporation of a sulfide ion at the center. While similar treatment using the analogous $\text{Cu}_3\text{Ir}^{\text{III}}_2$ complex with *fac*- $[\text{Ir}(\text{aet})_3]$ metalloligands, $[\text{Cu}_3\{\text{Ir}(\text{aet})_3\}_2]^{3+}$, produced the isostructural $\text{Cu}_6\text{Ir}^{\text{III}}_4$ decanuclear complex, $[\text{Cu}_6\text{S}\{\text{Ir}(\text{aet})_3\}_4]^{4+}$, the use of the $\text{Cu}_3\text{Rh}^{\text{III}}_2$ complex with *fac*- $[\text{Rh}(\text{apt})_3]$ metalloligands, $[\text{Cu}_3\{\text{Rh}(\text{apt})_3\}_2]^{3+}$ (apt = 3-amino-propanethiolate), resulted in the removal of one of the three Cu^{I} atoms from $\{\text{Cu}^{\text{I}}_3\}^{3+}$ to afford the $\text{Cu}_2\text{Rh}^{\text{III}}_2$ tetranuclear complex, $[\text{Cu}_2\{\text{Rh}(\text{apt})_3\}_2]^{2+}$.

Introduction

Since sulfide ions tend to form tight coordination bonds with copper(I) ions, the interaction between copper(I) and sulfide ions is crucial across several scientific fields, including materials science, environmental science, and biochemistry.^[1–3] While this interaction has long been applied to fabricate bulk Cu_xS semiconductors with various compositions and morphologies,^[1] in recent years, research has been performed to create atomically precise nanoclusters of copper(I) sulfide, which exhibit unique photophysical and catalytic properties.^[4] In 1994, Fenske and coworkers succeeded in preparing and crystallizing discrete copper(I) sulfide clusters protected by phosphine ligands, $[\text{Cu}_{12}\text{S}_6(\text{PEt}_3)_8]$ or $[\text{Cu}_{20}\text{S}_{10}(\text{PPh}_3)_8]$, by using $\text{S}(\text{SiMe}_3)_2$ as a

sulfide source.^[5] Their results indicated that a slight difference in substituent groups on phosphine ligands could regulate the nuclearity of the resulting copper(I) sulfide clusters. After the pioneering work by Fenske, various organic and organo-metallic ligands, such as phosphines,^[5,6] dithiophosphates,^[7] dithiocarbamates,^[8] thiolates,^[9] and thiometallates,^[10] were used as protecting ligands for creating copper(I) sulfide nanoclusters with high nuclearity. Yam et al. reported that treatment of the cyclic dicopper(I) complex, $[\text{Cu}_2(\text{dppm})_2]^{2+}$ (dppm = bis(diphenylphosphino)methane), with Na_2S produced the photoluminescent tetracopper(I) sulfide cluster, $[\text{Cu}_4(\mu_4\text{-S})(\text{dppm})_4]^{2+}$,^[11] here, two cyclic dicopper(I) molecules coalesced into the larger macrocyclic structure in $[\text{Cu}_4(\text{dppm})_4]^{4+}$ to accommodate a sulfide ion. Yam's work received increasing attention after the structural determination of nitrous oxide reductase because its active center had a flat tetranuclear $\{\text{Cu}_4(\mu_4\text{-S})\}^{2+}$ moiety, and its structure was similar to that in $[\text{Cu}_4(\mu_4\text{-S})(\text{dppm})_4]^{2+}$.^[12] Subsequently, Monkad et al. and Meyer et al. independently synthesized analogous $[\text{Cu}_4(\mu_4\text{-S})(\text{L})_4]$ -type clusters with N-donor ligands through sulfide-induced dimerization reactions of cyclic dicopper(I) precursors.^[13] While these findings showed the utility of sulfide ions for the structural transformation of copper(I) clusters, reports on the use of Na_2S , NaSH , and H_2S as sulfide sources are still limited to the transformation of dicopper(I) and tetracopper(I) precursors.^[12,14] This is mainly due to the strong binding of S^{2-} to copper(I) centers, which causes the decomposition of a copper(I) cluster into Cu_2S with a low solubility ($K_{\text{sp}} = 1.2 \times 10^{-49}$),^[15] the demetallation from copper(I) clusters to form Cu_2S has been applied to a luminescent sensor for detecting H_2S or S^{2-} .^[16] Thus, a rigid coordination system that can prevent the formation of Cu_2S is desirable to use in the structural transformation of copper(I) clusters by sulfide ions.

[a] Dr. Z. L. Goo, Dr. N. Yoshinari, Y. Yasukawa, K. Minami, Prof. T. Konno
Department of Chemistry
Graduate School of Science, Osaka University
Toyonaka, Osaka 560-0043 (Japan)
E-mail: nobuto@chem.sci.osaka-u.ac.jp
konno@chem.sci.osaka-u.ac.jp

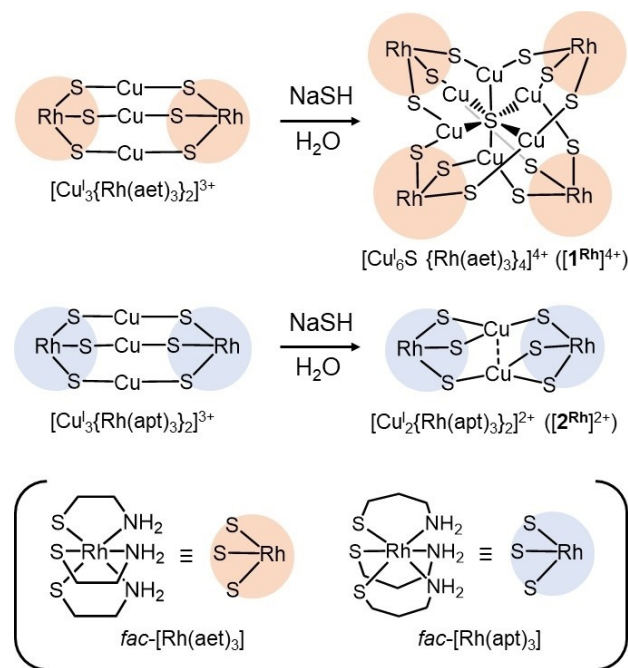
[b] Dr. Z. L. Goo
Department of Chemistry
Kindai University
Higashiosaka, Osaka, 577-8502 (Japan)

[c] Prof. T. Konno
Department of Chemistry
College of Science, National Taiwan Normal University
Taipei 11677 (Taiwan)

Supporting information for this article is available on the WWW under <https://doi.org/10.1002/asia.202400266>

© 2024 The Authors. Chemistry - An Asian Journal published by Wiley-VCH GmbH. This is an open access article under the terms of the Creative Commons Attribution License, which permits use, distribution and reproduction in any medium, provided the original work is properly cited.

Based on our continuing study on the utility of thiolato metal complexes as metalloligands,^[17] we recently found that the reactions of the octahedral rhodium(III) complexes, *fac*-[Rh(aet)₃] (aet = 2-aminoethanethiolate) and *fac*-[Rh(apt)₃] (apt = 3-aminopropanethiolate), with Ag⁺ in the presence of a sulfide source produced the water-soluble silver(I) sulfide clusters, [Ag₄₆S₁₃(M(aet)₃)₁₄]²⁰⁺ and [Ag₁₃S(Rh(apt)₃)₆]¹¹⁺, respectively.^[18,19] Encouraged by the successful creation of silver(I) sulfide clusters from the *fac*-[Rh(aet)₃] and *fac*-[Rh(apt)₃] metalloligands and S²⁻, together with the control of cluster sizes by changing the chelate-ring sizes (5-membered aet vs. 6-membered apt) in the metalloligands, in this study, we investigated the reactivities of [Cu₃{Rh(aet or apt)₃}₂]³⁺ toward S²⁻; each Cu₃Rh^{III}₂ pentanuclear complex has a triangular cluster moiety of {Cu₃}³⁺ supported by two *fac*-[Rh(aet or apt)₃] metalloligands.^[20] We found that treatment of [Cu₃{Rh(aet)₃}₂]³⁺ with NaSH produced a Cu₆Rh^{III}₄ decanuclear complex with an octahedral {Cu₆(μ₆-S)}⁴⁺ core, [Cu₆S{Rh(aet)₃}₄]⁴⁺ ([1^{Rh}]⁴⁺), accompanied by the dimerization of {Cu₃}³⁺ and the incorporation of a sulfide ion (Scheme 1). On the other hand, similar treatment using [Cu₃{Rh(apt)₃}₂]³⁺ was found to produce the Cu₂Rh^{III}₂ tetranuclear complex, [Cu₂{Rh(apt)₃}₂]²⁺ ([2^{Rh}]²⁺), due to the removal of one of three Cu^I atoms from {Cu₃}³⁺ by S²⁻. To our knowledge, this is the first copper(I) coordination system in which the structural expansion and contraction are induced by sulfide ions. The Cu₆Rh^{III}₄ decanuclear complex [Cu₆S{Rh(aet)₃}₄]⁴⁺ ([1^{Rh}]⁴⁺), analogous to [1^{Rh}]⁴⁺, which was produced from the newly prepared [Cu₃{Rh(aet)₃}₂]³⁺ and NaSH, is also reported.



Scheme 1. Synthetic routes of [1^{Rh}]⁴⁺ and [2^{Rh}]²⁺ from *fac*-[Rh(aet)₃] and *fac*-[Rh(apt)₃], respectively.

Results and Discussion

Reaction of [Cu₃{Rh(aet)₃}₂]³⁺ with NaSH

Treatment of [Cu₃{Rh(aet)₃}₂](BF₄)₃ with NaSH in degassed water caused an immediate color change from yellow to orange without precipitation. From the reaction solution, an orange crystalline powder ([1^{Rh}](BF₄)₄) was isolated by adding NaBF₄. X-ray fluorescence measurements indicated that the product contained Rh and Cu atoms in a 2:3 ratio. The retention of the +1 oxidation state of the copper centers was indicated by the absence of visible d-d transition bands in the absorption spectrum (Figure 1). In the ¹H NMR spectrum of degassed D₂O, [1^{Rh}](BF₄)₄ gave broad, complicated signals due to the methylene (δ 2.2–3.2 ppm) and amine (δ 3.8–4.7 ppm) protons of the aet ligands; these signals were located at magnetic fields higher than the corresponding signals for [Cu₃{Rh(aet)₃}₂](BF₄)₃·CH₃CN (Figure S1). The upfield shift of the signals was caused by the increase in electron density on the aet ligands, indicating the binding of electron-rich S²⁻ to the Cu^I centers. In addition, the elemental analytical data of [1^{Rh}](BF₄)₄ matched well with the formula for the 2:1 adduct of [Cu₃{Rh(aet)₃}₂]³⁺ and S²⁻.

An attempt to recrystallize [1^{Rh}](BF₄)₄ from degassed water in a glass vial resulted in the isolation of microcrystals of [1^{Rh}](BF₄)₂(SiF₆); its structure was determined by single-crystal X-ray analysis. The asymmetric unit of [1^{Rh}](BF₄)₂(SiF₆) contained one complex cation and two BF₄⁻ anions, together with one SiF₆²⁻ anion that was assumed to be formed *in situ* by the reaction of BF₄⁻ with the glass vial (Figure S2).^[21] The presence of these anions indicate the tetracationic state of the complex. As shown in Figure 2, the complex cation has an S²⁻ ion at the center, which is bound by six Cu^I atoms to form a distorted octahedral core of {Cu₆S}⁴⁺ (av. Cu–S²⁻ = 2.26 Å, av. *trans*-Cu–S²⁻–Cu = 158.6°). The {Cu₆S}⁴⁺ core is converted by four *fac*-[Rh(aet)₃] units in a tetrahedral arrangement through thiolato groups of aet (av. Cu–S_{aet} = 2.24 Å), completing the S-bridged Cu₆Rh^{III}₄ decanuclear

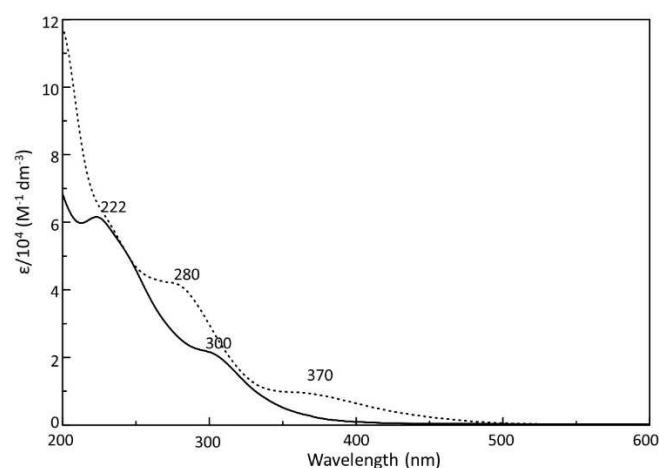


Figure 1. Absorption spectra of [1^{Rh}](BF₄)₄ (dotted line) and [1^H](BF₄)₄ (solid line) in water.

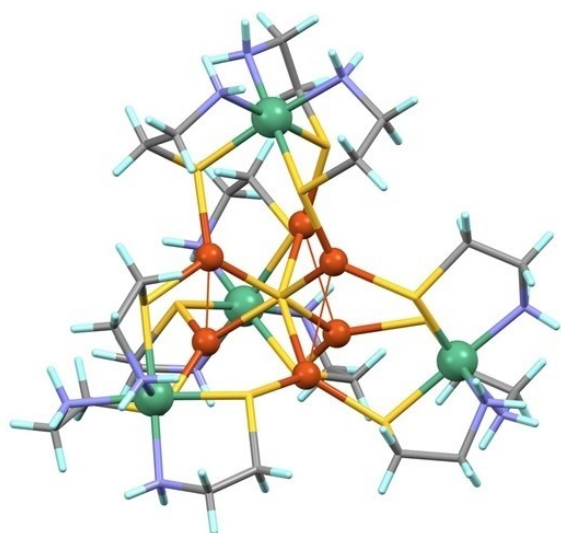


Figure 2. Perspective view of $[1^{\text{Rh}}]^{4+}$. One of the disordered parts is illustrated. Color code: Rh: blue–green, Cu: brown, S: yellow, N: blue, C: gray, H: pale blue.

structure in $[\text{Cu}_6\text{S}\{\text{Rh}(\text{aet})_3\}_4]^{4+}$ ($[1^{\text{Rh}}]^{4+}$). In $[1^{\text{Rh}}]^{4+}$, the Cu^{I} centers are each situated in an ideal trigonal-planar geometry coordinated by two S atoms from two different $\text{fac}[\text{Rh}(\text{aet})_3]$ units and an S^{2-} ion (av. $\text{S}-\text{Cu}-\text{S}=119.7^\circ$). Two short $\text{Cu}\cdots\text{Cu}$ contacts (av. 2.77 \AA) are present, and their distances are less than the sum of the van der Waals radii of two Cu atoms (2.80 \AA),^[22] indicating the occurrence of cuprophilic interactions in the $\{\text{Cu}_6\text{S}\}^{4+}$ core.^[23] Considering the Δ and Λ chiral configurations for each $\text{fac}[\text{Rh}(\text{aet})_3]$ unit, five stereoisomers, Δ_4 , $\Delta_3\Lambda$, $\Delta_2\Lambda_2$, $\Delta\Lambda_3$, and Λ_4 , are possible for $[\text{Cu}_6\text{S}\{\text{Rh}(\text{aet})_3\}_4]^{4+}$. Since $[1^{\text{Rh}}](\text{BF}_4)_2(\text{SiF}_6)$ was crystallized in the achiral space group of $P2_1/c$ with the $\Delta\Lambda_3$ isomer in the asymmetric unit (Figure S2), the product is a racemic compound composed of a pair of enantiomers of $\Delta_3\Lambda-[1^{\text{Rh}}]^{4+}$ and $\Lambda\Delta_3-[1^{\text{Rh}}]^{4+}$ with C_3 symmetry.^[24] The broad, complicated proton signals in the ^1H NMR spectrum of $[1^{\text{Rh}}](\text{BF}_4)_4$ are consistent with those of the racemic compounds of the $\Delta\Lambda_3$ and $\Delta_3\Lambda$ isomers, which possess four sets of chemically inequivalent aet ligands. Note that the overall $\text{Cu}_6\text{Rh}^{III}_4$ structure in $[1^{\text{Rh}}]^{4+}$ is similar to that in the anionic $[\text{Cu}_6\text{S}\{\text{Rh}(\text{L-cysteinate})_3\}_4]^{8-}$,^[14] which was previously synthesized by the insertion reaction of S^{2-} into the empty $\{\text{Cu}_4\}^{4+}$ core of $[\text{Cu}_4\{\text{Rh}(\text{L-cysteinate})_3\}_4]^{8-}$.^[25]

Reaction of $[\text{Cu}_3\{\text{Ir}(\text{aet})_3\}_2]^{3+}$ with NaSH

To investigate the utility of the sulfide-induced dimerization reaction for other coordination compounds, we prepared a new $\text{Cu}^{\text{I}}\text{Ir}^{\text{III}}_2$ pentanuclear complex, $[\text{Cu}_3\{\text{Ir}(\text{aet})_3\}_2](\text{BF}_4)_3$, analogous to $[\text{Cu}_3\{\text{Rh}(\text{aet})_3\}_2](\text{BF}_4)_3$; this was subsequently reacted with NaSH under the same conditions. This reaction produced a deep yellow solution, from which yellow block crystals ($[1^{\text{Ir}}](\text{BF}_4)_4$) suitable for X-ray crystallography were obtained. The ^1H NMR spectrum of $[1^{\text{Ir}}](\text{BF}_4)_4$ in degassed D_2O showed broad, compli-

cated proton signals, as in the case of $[1^{\text{Rh}}](\text{BF}_4)_4$ (Figure S3). The elemental and fluorescence X-ray analyses of $[1^{\text{Ir}}](\text{BF}_4)_4$ were consistent with the chemical formula for $[\text{Cu}_6\text{S}\{\text{Ir}(\text{aet})_3\}_4](\text{BF}_4)_4$, and its structure was established by single-crystal X-ray analysis. The overall structure of $[1^{\text{Ir}}]^{4+}$ was the same as that of $[1^{\text{Rh}}]^{4+}$, except for the presence of Ir^{III} atoms in place of Rh^{III} atoms in $[1^{\text{Rh}}]^{4+}$ (Figures 3 and S4). In addition, the geometrical parameters of the Cu^{I} centers (av. $\text{Cu}-\text{S}^{2-}=2.27 \text{ \AA}$, av. $\text{trans-Cu}-\text{S}^{2-}-\text{Cu}=154.4^\circ$, av. $\text{Cu}-\text{S}_{\text{aet}}=2.25 \text{ \AA}$, $\text{Cu}\cdots\text{Cu}=2.72 \text{ \AA}$) in $[1^{\text{Ir}}]^{4+}$ were very similar to those in $[1^{\text{Rh}}]^{4+}$.

Here, the solid samples of $[\text{Cu}_3\{\text{Ir}(\text{aet})_3\}_2](\text{BF}_4)_3$ and $[1^{\text{Ir}}](\text{BF}_4)_4$ are emissive at low temperature, while no emission was observed for $[\text{Cu}_3\{\text{Rh}(\text{aet})_3\}_2](\text{BF}_4)_3$ and $[1^{\text{Rh}}](\text{BF}_4)_4$ under the same conditions. This occurred because the d-d absorptions, which are in the visible region for $[\text{Cu}_3\{\text{Rh}(\text{aet})_3\}_2](\text{BF}_4)_3$ and $[1^{\text{Rh}}](\text{BF}_4)_4$, shifted to the higher energy side for $[\text{Cu}_3\{\text{Ir}(\text{aet})_3\}_2](\text{BF}_4)_3$ and $[1^{\text{Ir}}](\text{BF}_4)_4$ (Figure 1) and prevented the energy transfer to the nonemissive d-d excited states. In the emission spectrum at 77 K , $[1^{\text{Ir}}](\text{BF}_4)_4$ exhibited a weak band at 660 nm with a quantum yield of less than 0.1% (Figure 4).

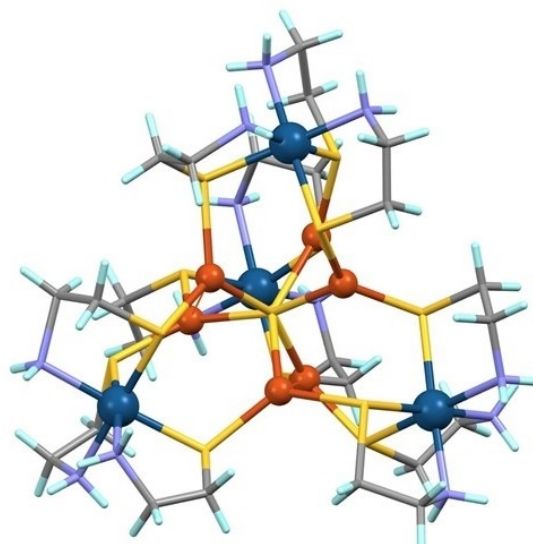


Figure 3. Perspective view of $[1^{\text{Ir}}]^{4+}$. One of the disordered parts is illustrated. Color code: Ir: dark cyan, Cu: brown, S: yellow, N: blue, C: gray, H: pale blue.

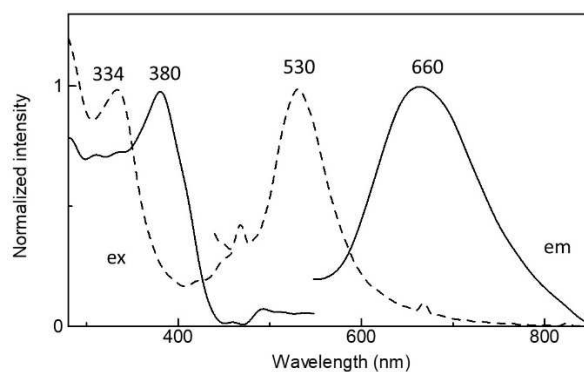


Figure 4. Excitation (ex) and emission (em) spectra of $[\text{Cu}_3\{\text{Ir}(\text{aet})_3\}_2](\text{BF}_4)_3 \cdot \text{CH}_3\text{CN} \cdot \text{H}_2\text{O}$ (dashed line) and $[1^{\text{Ir}}](\text{BF}_4)_4$ (solid line) in the solid-state at 77 K .

A corresponding emission band was observed for $[\text{Cu}_3\{\text{Ir}(\text{aet})_3\}_2](\text{BF}_4)_3$ at 530 nm with a quantum yield of 1.3% (Figure 4). Thus, the structural conversion from $[\text{Cu}_3\{\text{Ir}(\text{aet})_3\}_2](\text{BF}_4)_3$ to $[\text{I}^{\text{Ir}}](\text{BF}_4)_4$ resulted in a large redshift of the emission band, as well as partial quenching of the emission which is most likely due to the slight redshift of the d-d absorptions. Since the DFT calculations revealed that the HOMO and LUMO for $[\text{Cu}_3\{\text{Ir}(\text{aet})_3\}_2]^{3+}$ are dominated by thiolate groups and a $\{\text{Cu}'_3\}$ moiety, respectively, and those of $[\text{I}^{\text{Ir}}]^{4+}$ are dominated by a $\{\text{Cu}_6\text{S}\}^{4+}$ moiety and Ir^{III} centers, respectively (Figure S5), the large redshift of the emission was caused by the changes in the HOMO and LUMO to have an intracuster $\{\text{Cu}_6\text{S}\}$ -to-Ir charge transfer transition with a lower energy. The emission energy for $[\text{I}^{\text{Ir}}](\text{BF}_4)_4$ is also lower than that of the previously reported tetranuclear $\{\text{Cu}_4\text{S}\}^{2+}$ complexes $[\text{Cu}_4(\mu_4\text{-S})(\text{dppa})_4](\text{PF}_6)_2$ ($\lambda_{\text{em}} = 571 \text{ nm}$)^[11a] and $[\text{Cu}_4(\mu_4\text{-S})(\text{dppm})_4](\text{PF}_6)_2$ ($\lambda_{\text{em}} = 606 \text{ nm}$)^[11c] presumably because of the presence of cuprophilic interactions that lowered the LUMO in $[\text{I}^{\text{Ir}}](\text{BF}_4)_4$.

Reaction of $[\text{Cu}_3\{\text{Rh}(\text{apt})_3\}_2]^{3+}$ with NaSH

We also investigated whether a similar sulfide-induced dimerization occurred for $[\text{Cu}_3\{\text{Rh}(\text{apt})_3\}_2](\text{BF}_4)_3$, which is composed of *fac*- $[\text{Rh}(\text{apt})_3]$ units with six-membered N,S-chelate rings of apt. Treatment of $[\text{Cu}_3\{\text{Rh}(\text{apt})_3\}_2](\text{BF}_4)_3$ with NaSH under similar conditions immediately produced an orange suspension.^[26] After filtration, an orange crystalline powder ($[\text{2}^{\text{Rh}}](\text{BF}_4)_2$) was isolated from the filtrate by adding NaBF_4 .^[27] The ^1H NMR spectral feature of $[\text{2}^{\text{Rh}}](\text{BF}_4)_2$ in degassed methanol- d_4 was different from that of the starting complex of $[\text{Cu}_3\{\text{Rh}(\text{apt})_3\}_2](\text{BF}_4)_3$ in D_2O , producing broad signals at chemical shifts different from the sharp signals of $[\text{Cu}_3\{\text{Rh}(\text{apt})_3\}_2](\text{BF}_4)_3$ (Figure S6). X-ray fluorescence and elemental analyses indicated that $[\text{2}^{\text{Rh}}](\text{BF}_4)_2$ is a 1:1 adduct of Cu^{I} and *fac*- $[\text{Rh}(\text{apt})_3]$ with a lack of S^{2-} .

Single crystals of $[\text{2}^{\text{Rh}}](\text{BF}_4)_2 \cdot 2\text{MeOH}$ were obtained by recrystallizing the orange powder of $[\text{2}^{\text{Rh}}](\text{BF}_4)_2$ from dry methanol. X-ray analysis of this sample revealed the presence of half a complex-cation that lied on the crystallographic inversion center, one BF_4^- anion, and one solvated methanol in the asymmetric unit (Figure S7). The dicationic state of $[\text{2}^{\text{Rh}}]^{2+}$ was indicated by the 1:2 ratio of complex cations and BF_4^- anions. As shown in Figure 5, the entire complex-cation contains two *fac*- $[\text{Rh}(\text{apt})_3]$ units that are spanned by two Cu^{I} atoms, forming the S-bridged $\text{Cu}'_2\text{Rh}^{\text{III}}_2$ tetranuclear structure in $[\text{Cu}'_2\{\text{Rh}(\text{apt})_3\}_2]^{2+}$. The formation of the $\text{Cu}'_2\text{Rh}^{\text{III}}_2$ structure indicated the removal of one of three Cu^{I} atoms from $[\text{Cu}_3\{\text{Rh}(\text{apt})_3\}_2]^{3+}$ in the course of the reaction with S^{2-} . To our knowledge, the partial removal of Cu^{I} from copper(I) species by S^{2-} is unprecedented, while the complete removal of Cu_2S has commonly been observed.^[16] In $[\text{2}^{\text{Rh}}]^{2+}$, each *fac*- $[\text{Rh}(\text{apt})_3]$ unit is bound to two Cu^{I} atoms through three thiolato groups in a chelate-bridging mode. This bridging is different from the bridging mode found in $[\text{1}^{\text{Rh}}]^{4+}$, in which each *fac*- $[\text{Rh}(\text{aet})_3]$ unit is bound to three different Cu^{I} atoms.

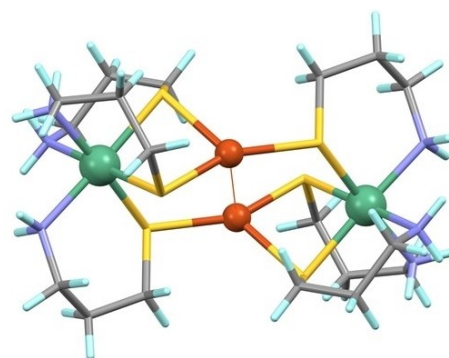


Figure 5. Perspective view of $[\text{2}^{\text{Rh}}]^{2+}$. Color code: Rh: blue–green, Cu: brown, S: yellow, N: blue, C: gray, H: pale blue.

As in $[\text{1}^{\text{Rh}}]^{4+}$, each Cu^{I} center in $[\text{2}^{\text{Rh}}]^{2+}$ has a trigonal-planar geometry. This geometry in $[\text{2}^{\text{Rh}}]^{2+}$ is completed by the coordination of two S atoms from one *fac*- $[\text{Rh}(\text{apt})_3]$ unit and one S atom from the other *fac*- $[\text{Rh}(\text{apt})_3]$ unit (av. $\text{Cu}-\text{S} = 2.27 \text{ \AA}$). The $\text{Cu}^{\text{I}}\cdots\text{Cu}^{\text{I}}$ distance in $[\text{2}^{\text{Rh}}]^{2+}$ is 2.68 \AA , indicating the presence of a cuprophilic interaction stronger than that found in $[\text{1}^{\text{Rh}}]^{4+}$. The two *fac*- $[\text{Rh}(\text{apt})_3]$ units in $[\text{2}^{\text{Rh}}]^{2+}$ possess opposite chiral configurations to form the $\Delta\Lambda$ meso isomer. Since the starting $[\text{Cu}_3\{\text{Rh}(\text{apt})_3\}_2]^{3+}$ was the Δ_2/Λ_2 racemic isomer,^[20] the partial demetallation by S^{2-} was accompanied by the scrambling of the *fac*- $[\text{Rh}(\text{apt})_3]$ units to produce the meso isomer for $[\text{2}^{\text{Rh}}]^{2+}$. A similar demetallation reaction of $[\text{Cu}_3\{\text{Rh}(\text{apt})_3\}_2]^{3+}$ was observed when the aqueous solution was kept under aerobic conditions. In this case, however, the product was the Δ_2/Λ_2 racemic isomer of the $\text{Cu}'\text{Cu}^{\text{II}}\text{Rh}^{\text{III}}_2$ tetranuclear complex, $[\text{Cu}'\text{Cu}^{\text{II}}\{\text{Rh}(\text{apt})_3\}_2]^{3+}$, in which two *fac*- $[\text{Rh}(\text{apt})_3]$ units with the same chiral configuration are spanned by linear Cu^{I} and square-planar Cu^{II} centers.^[20]

Concluding Remarks

We showed that the $\text{Cu}'_3\text{Rh}^{\text{III}}_2$ pentanuclear complex with 5-membered chelate rings of aet, $[\text{Cu}_3\{\text{Rh}(\text{aet})_3\}_2]^{3+}$, reacted with NaSH in water to construct the $\text{Cu}'_6\text{Rh}^{\text{III}}_4$ decanuclear structure in $[\text{Cu}'_6\text{S}\{\text{Rh}(\text{aet})_3\}_4]^{4+}$ ($[\text{1}^{\text{Rh}}]^{4+}$); here, the octahedral $\{\text{Cu}_6\text{S}\}^{4+}$ core was supported by four *fac*- $[\text{Rh}(\text{aet})_3]$ metal-ligands that adopted a bridging coordination mode. The same result was obtained when the analogous $\text{Cu}'_3\text{Ir}^{\text{III}}_2$ complex, $[\text{Cu}_3\{\text{Ir}(\text{aet})_3\}_2]^{3+}$, was reacted with NaSH, and this reaction produced the isostructural decanuclear structure in $[\text{Cu}'_6\text{S}\{\text{Ir}(\text{aet})_3\}_4]^{4+}$ ($[\text{1}^{\text{Ir}}]^{4+}$). On the other hand, a similar reaction using the corresponding $\text{Cu}'_3\text{Rh}^{\text{III}}_2$ complex with 6-membered chelate rings of apt, $[\text{Cu}_3\{\text{Rh}(\text{apt})_3\}_2]^{3+}$, produced the $\text{Cu}'_2\text{Rh}^{\text{III}}_2$ tetranuclear structure in $[\text{Cu}'_2\{\text{Rh}(\text{apt})_3\}_2]^{2+}$ ($[\text{2}^{\text{Rh}}]^{2+}$); here, two trigonal-planar Cu^{I} centers were supported by two terminal *fac*- $[\text{Rh}(\text{apt})_3]$ metalloligands that adopted a chelate-bridging mode.^[28] Thus, the small difference in the chelate ring sizes (5-membered vs. 6-membered) caused the large difference in the reactivities of the $\text{Cu}'_3\text{Rh}^{\text{III}}_2$ complexes toward S^{2-} ; these results showed the dimerization of the

$\text{Cu}^{\text{I}}_3\text{Rh}^{\text{III}}_2$ structure assisted by the inclusion of an S^{2-} ion for $[\text{Cu}_3\{\text{Rh}(\text{aet})_3\}_2]^{3+}$ vs. the demetallation of one of three Cu^{I} centers from the $\text{Cu}^{\text{I}}_3\text{Rh}^{\text{III}}_2$ structure for $[\text{Cu}_3\{\text{Rh}(\text{apt})_3\}_2]^{3+}$. The octahedral $\{\text{Cu}_6\text{S}\}^{4+}$ core is difficult to cover with *fac*- $[\text{Rh}(\text{apt})_3]$ metalloligands because of the steric crowding among the metalloligands bearing the bulky, 6-membered chelate rings. In addition, *fac*- $[\text{Rh}(\text{apt})_3]$ prefers to chelate a metal center rather than bridging three metal centers because of the relative direction of three lone pairs from three thiolato groups in *fac*- $[\text{Rh}(\text{apt})_3]$ (Figure S8).^[19,29] Thus, steric crowding, together with the preferential coordination mode for *fac*- $[\text{Rh}(\text{apt})_3]$, led to the conversion of $[\text{Cu}_3\{\text{Rh}(\text{apt})_3\}_2]^{3+}$ to $[\text{2}^{\text{Rh}}]^{2+}$ via the removal of a Cu^{I} center by S^{2-} . Notably, the replacement of Rh^{III} centers in $[\text{Cu}_3\{\text{Rh}(\text{aet})_3\}_2]^{3+}$ and $[\text{1}^{\text{Rh}}]^{4+}$ by Ir^{III} caused this system to be photoluminescent, which enabled the investigation of the photophysical changes accompanied by structural conversion; the conversion from $[\text{Cu}_3\{\text{Ir}(\text{aet})_3\}_2]^{3+}$ to $[\text{1}^{\text{Ir}}]^{4+}$ was found to cause an appreciable redshift of the emission band. Finally, our study demonstrated that sulfide-induced transformation is a practical approach for the structural expansion/contraction of copper(I) coordination compounds, which can modify their physicochemical properties. We are currently investigating whether the sulfide-induced transformation is applicable for other multinuclear complexes.

Experimental Section

Starting Complexes

The $\text{Cu}^{\text{I}}_3\text{Rh}^{\text{III}}_2$ complexes $[\text{Cu}_3\{\text{Rh}(\text{aet})_3\}_2](\text{BF}_4)_3 \cdot \text{CH}_3\text{CN}$ and $[\text{Cu}_3\{\text{Rh}(\text{apt})_3\}_2](\text{BF}_4)_3 \cdot 4\text{H}_2\text{O}$ were synthesized according to procedures in the literature.^[20] The $\text{Cu}^{\text{I}}_3\text{Ir}^{\text{III}}_2$ complex $[\text{Cu}_3\{\text{Ir}(\text{aet})_3\}_2](\text{BF}_4)_3 \cdot \text{CH}_3\text{CN}$ (Figure S9) was newly synthesized by a procedure similar to that employed for $[\text{Cu}_3\{\text{Rh}(\text{aet})_3\}_2](\text{BF}_4)_3 \cdot \text{CH}_3\text{CN}$ (see the Supporting Information). All reactions were carried out under N_2 with standard Schlenk techniques.

Preparation of $[\text{Cu}_6\text{S}\{\text{Rh}(\text{aet})_3\}_4](\text{BF}_4)_4$ ($[\text{1}^{\text{Rh}}](\text{BF}_4)_4$)

To a yellow solution containing 0.12 g (0.105 mmol) of $[\text{Cu}_3\{\text{Rh}(\text{aet})_3\}_2](\text{BF}_4)_3 \cdot \text{CH}_3\text{CN}$ in 14 mL of degassed water was added 0.52 mL of 0.2 M NaSH (0.104 mmol). The resulting orange solution was stirred at room temperature for 2 h under N_2 . After removing a negligible amount of precipitate *via* Celite filtration, 3 mL of saturated aqueous NaBF_4 was added to the filtrate. The mixture was left in the dark for 6 h to yield an orange crystalline powder of $[\text{1}^{\text{Rh}}](\text{BF}_4)_4$; these crystals were collected by filtration. Yield: 73 mg (65%). Anal Calcd. for $[\text{Cu}_6\text{S}\{\text{Rh}(\text{aet})_3\}_4](\text{BF}_4)_4 \cdot 6\text{H}_2\text{O} = \text{C}_{24}\text{H}_{86}\text{B}_4\text{Cu}_6\text{F}_{16}\text{N}_{12}\text{O}_6\text{Rh}_4\text{S}_1$: C, 13.14; H, 3.86; N, 7.66%. Found: C, 13.29; H, 3.62; N, 7.69%.

The recrystallization of $[\text{1}^{\text{Rh}}](\text{BF}_4)_4$ from degassed water containing NaBF_4 produced a very small amount of orange single crystals of $[\text{1}^{\text{Rh}}](\text{BF}_4)_2(\text{SiF}_6)$ suitable for single-crystal X-ray analysis.

Preparation of $[\text{Cu}_6\text{S}\{\text{Ir}(\text{aet})_3\}_4](\text{BF}_4)_4$ ($[\text{1}^{\text{Ir}}](\text{BF}_4)_4$)

To a pale yellow solution containing 0.12 g (0.09 mmol) of $[\text{Cu}_3\{\text{Ir}(\text{aet})_3\}_2](\text{CH}_3\text{CN})(\text{BF}_4)_3$ in 14 mL of degassed water was added

0.44 mL of 0.2 M NaSH (0.09 mmol). The resulting deep yellow solution was stirred at room temperature for 2 h under N_2 . After removing a small amount of precipitate *via* Celite filtration, 2 mL of saturated aqueous NaBF_4 was added to the filtrate. The mixture was left in the dark for 6 h to yield yellow crystals of $[\text{1}^{\text{Ir}}](\text{BF}_4)_4$ suitable for single-crystal X-ray structural analysis; the crystals were collected by filtration. Yield: 43 mg (37%). Anal Calcd. for $[\text{Cu}_6\text{S}\{\text{Ir}(\text{aet})_3\}_4](\text{BF}_4)_4 \cdot 7\text{H}_2\text{O} = \text{C}_{24}\text{H}_{86}\text{B}_4\text{Cu}_6\text{F}_{16}\text{Ir}_4\text{N}_{12}\text{O}_7\text{S}_1$: C, 11.22; H, 3.37; N, 6.54%. Found: C, 11.22; H, 3.44; N, 6.60%.

Preparation of $[\text{Cu}_2\{\text{Rh}(\text{apt})_3\}_2](\text{BF}_4)_2$ ($[\text{2}^{\text{Rh}}](\text{BF}_4)_2$)

To a yellow solution containing 0.06 g (0.047 mmol) of $[\text{Cu}_3\{\text{Rh}(\text{apt})_3\}_2](\text{BF}_4)_3 \cdot 4\text{H}_2\text{O}$ in 10 mL of degassed water was added 0.12 mL of 0.2 M NaSH (0.024 mmol). The resulting suspension was stirred at room temperature for 30 min under N_2 . After removing a small amount of precipitate *via* Celite filtration, 200 mg of NaBF_4 was added to the filtrate. The mixture was left in the dark for 20 min to yield an orange powder; this powder was collected by filtration. Yield: 24 mg (47%). Anal Calcd. for $[\text{Cu}_2\{\text{Rh}(\text{apt})_3\}_2](\text{BF}_4)_2 \cdot 2\text{H}_2\text{O} = \text{C}_{18}\text{H}_{52}\text{B}_2\text{Cu}_2\text{F}_8\text{N}_6\text{O}_2\text{Rh}_2\text{S}_6$: C, 19.95; H, 4.84; N, 7.76%. Found: C, 19.88; H, 4.68; N, 7.57%.

Recrystallization of the orange powder from dry methanol produced orange-yellow crystals of $[\text{2}^{\text{Rh}}](\text{BF}_4)_2 \cdot 2\text{MeOH}$; these were suitable for single-crystal X-ray analysis.

Physical Measurements

UV-Vis spectra were recorded with a JASCO V-660 spectrometer. IR spectra were measured with a JASCO FT/IR-4100 infrared spectrophotometer using the KBr method. Elemental analysis (C, H, N) was performed on a YANACO CHN Corder MT-5. X-ray fluorescence measurements were performed with a SHIMADZU EDX-7000 spectrometer. ^1H NMR spectra were recorded with a JEOL EXA 500 (500 MHz) spectrometer in D_2O and methanol- d_4 with sodium 4,4'-dimethyl-4-silapentane-1-sulfonate (DSS) and tetramethylsilane (TMS) as the internal standards, respectively. The photoluminescence spectra were recorded with a JASCO FP-8500 spectrometer at 77 K. For the powder XRD (PXRD) pattern, a dry sample was packed into glass capillary tubes, and the measurements were performed at the BL02B2 beamline at SPring-8.^[30] ESI mass spectra were measured with a Bruker MicrOTOF-II or Waters X500R in methanol/water in a positive mode. DFT calculation was performed using Gaussian 09 based on the B3LYP functional and LANL2DZ basis set.^[31]

X-ray Structural Determinations

Single-crystal X-ray diffraction measurements for $[\text{Cu}_3\{\text{Ir}(\text{aet})_3\}_2](\text{BF}_4)_2 \cdot \text{CH}_3\text{CN} \cdot \text{H}_2\text{O}$ were performed using a Rigaku FR-E Superbright rotating-anode X-ray source with a Mo target equipped with a Rigaku RAXIS VII imaging plate as a detector at 200 K. X-ray diffraction measurements for $[\text{1}^{\text{Ir}}](\text{BF}_4)_4$ and $[\text{2}^{\text{Rh}}](\text{BF}_4)_2 \cdot 2\text{CH}_3\text{OH}$ were performed on a RIGAKU XtaLAB Synergy Custom X-ray diffractometer equipped with a HyPix-6000HE hybrid photon counting detector and a Rigaku VariMax rotating-anode X-ray source with a Mo target. X-ray diffraction measurements of $[\text{1}^{\text{Rh}}](\text{BF}_4)_2(\text{SiF}_6)$ were carried out using a PILATUS3 X CdTe 1 M detector with a synchrotron X-ray source at the BL02B1 beamline at SPring-8. For all crystals, the intensity data were collected in ω -scan mode, and empirical absorption corrections were applied. All structures were solved by direct methods using SHELXS or SHELXT.^[32] The structure refinements were carried out using full-matrix least squares in SHELXL.^[32] All calculations were

performed using the Olex2 software package.^[33] All nonhydrogen atoms were refined anisotropically, while hydrogen atoms were placed at the calculated positions using a riding model. For $[1^{\text{Rh}}](\text{BF}_4)_2(\text{SiF}_6)$ and $[1^{\text{Ir}}](\text{BF}_4)_4$, some of the *fac*- $[\text{M}(\text{aet})_3]$ ($\text{M} = \text{Rh}^{\text{III}}$, Ir^{III}) units and Cu atoms were disordered, and their occupancy factors were refined. The disordered parts were refined using the EADP, RIGU, DFIX, SIMU, and ISOR commands. For $[2^{\text{Rh}}](\text{BF}_4)_2$, ISOR restraints were applied for one N and one C atom to regulate the thermal ellipsoids. The crystallographic data are summarized in Table S1.^[34]

Supporting Information

The authors have cited additional references within the Supporting Information.^[35]

Acknowledgements

This work was supported by JSPS KAKENHI (Grant No. 19K05496 and 21J11148). The synchrotron radiation experiments were performed at the BL02B1 and BL02B2 beamlines of SPring-8 with the approval of the Japan Synchrotron Radiation Research Institute (JASRI) (Proposal Nos. 2022B1659 and 2022B1806). This work is the result of using research equipment shared in the MEXT Project for promoting public utilization of advanced research infrastructure (Program for supporting construction of core facilities) Grant No. JPMXS0441200023.

Conflict of Interests

The authors declare no conflict of interest.

Keywords: copper cluster · S ligand · sulfide ion · structural conversion · metalloligand

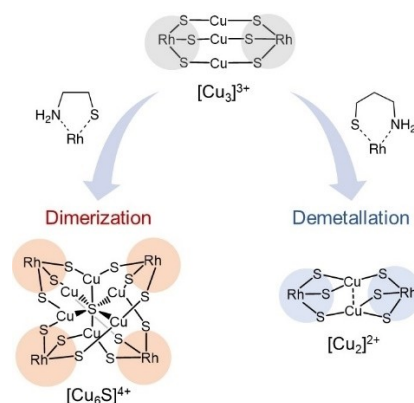
- [1] a) P. Roy, S. K. Srivastava, *CrystEngComm* **2015**, *17*, 7801–7815; b) C. Coughlan, M. Ibáñez, O. Dobrozhan, A. Singh, A. Cabot, K. Ryan, *Chem. Rev.* **2017**, *117*, 5865–6109; c) Y. Guo, Q. Wu, Y. Li, N. Lu, K. Mao, Y. Bai, J. Zhao, J. Wang, X. C. Zen, *Nanoscale Horiz.* **2019**, *4*, 223–230.
- [2] J. T. Rubino, K. J. Franz, *J. Inorg. Biochem.* **2012**, *107*, 129–143.
- [3] A. P. Chandra, A. R. Gerson, *Adv. Colloid Interface Sci.* **2009**, *145*, 97–110.
- [4] S. Dehnen, A. Eichhöfer, D. Fenske, *Eur. J. Inorg. Chem.* **2002**, *2002*, 279–317.
- [5] S. Dehnen, A. Schäfer, D. Fenske, R. Ahlrichs, *Angew. Chem. Int. Ed.* **1994**, *33*, 746–749.
- [6] a) M.-L. Fu, I. Issac, D. Fenske, O. Fuhr, *Angew. Chem. Int. Ed.* **2010**, *49*, 6899–6903; b) S. Bestgen, O. Fuhr, P. W. Roesky, D. Fenske, *Dalton Trans.* **2016**, *45*, 14907–14910; c) S. Dehnen, D. Fenske, A. C. Deveson, *J. Cluster Sci.* **1996**, *7*, 351–369; d) S. Dehnen, D. Fenske, *Chem. Eur. J.* **1996**, *2*, 1407–1416.
- [7] C. W. Liu, T. Stubbs, R. J. Staples, J. P. Fackler Jr., *J. Am. Chem. Soc.* **1995**, *117*(38), 9778–9779.
- [8] a) K. K. Chakrahari, R. P. B. Silalahi, J.-H. Liao, S. Kahlal, Y.-C. Liu, J.-F. Lee, M.-H. Chiang, J.-Y. Saillard, C. W. Liu, *Chem. Sci.* **2018**, *9*, 6785–6795; b) R. P. B. Silalahi, T.-H. Chiu, H. Liang, S. Kahlal, J.-Y. Saillard, C. W. Liu, *Chem. Commun.* **2023**, *59*, 9638–9641.
- [9] a) S. Schneider, J. A. S. Roberts, M. R. Salata, T. J. Marks, *Angew. Chem. Int. Ed.* **2006**, *45*, 1733–1736; b) Y. Lee, A. A. N. Sarjeanta, K. D. Karlin, *Chem. Commun.* **2006**, 621–623; c) A. Baghdasaryan, C. Besnard, L. M. L. Daku, T. Delgado, T. Burgi, *Inorg. Chem.* **2020**, *59*, 2200–2208; d) Y.-J. Cheng, R.-R. Wu, J.-Q. Zhao, E.-X. Chen, X. Zhou, Y. Dai, H.-L. Zheng, Q. Lin, *Cryst. Growth Des.* **2023**, *23*, 5421–5427.
- [10] P. Lin, X.-T. Wu, L. Chen, L.-M. Wu, W.-X. Du, *Polyhedron* **2000**, *19*, 2189–2193.
- [11] a) V. W.-W. Yam, W.-K. Lee, T.-F. Lai, *J. Chem. Soc. Chem. Commun.* **1993**, 1571–1573; b) V. W.-W. Yam, K. K.-W. Lo, W. K.-M. Fung, C.-R. Wang, *Coord. Chem. Rev.* **1998**, *171*, 17–41; c) C.-H. Lam, W. K. Tang, V. W.-W. Yam, *Inorg. Chem.* **2023**, *62*, 1942–1949.
- [12] a) K. Brown, M. Tegoni, M. Prudencio, A. S. Pereira, S. Besson, J. J. Moura, I. Moura, C. Cambillau, *Nat. Struct. Biol.* **2000**, *7*, 191–195; b) E. I. Solomon, R. Sarangi, J. S. Woertink, A. J. Augustine, J. Yoon, S. Ghosh, *Acc. Chem. Res.* **2007**, *40*, 581–591; c) P. Chen, S. I. Gorelsky, S. Ghosh, E. I. Solomon, *Angew. Chem. Int. Ed.* **2004**, *43*, 4132–4140.
- [13] a) B. J. Johnson, W. E. Antholine, S. V. Lindeman, N. P. Mankad, *Chem. Commun.* **2015**, *51*, 11860–11863; b) B. J. Johnson, W. E. Antholine, S. V. Lindeman, M. J. Graham, N. P. Mankad, *J. Am. Chem. Soc.* **2016**, *138*, 13107–13110; c) Y. Liu, S. Chatterjee, G. E. Cutsail III, S. Peredkov, S. K. Gupta, S. Dechert, S. DeBeer, F. Meyer, *J. Am. Chem. Soc.* **2023**, *145*, 18477–18486.
- [14] Y. Fukuda, N. Yoshinari, K. Yamagami, T. Konno, *Chem. Commun.* **2021**, *57*, 5386–5389.
- [15] S. Licht, *J. Electrochem. Soc.* **1988**, *135*, 2971–2975.
- [16] a) J. Li, C. Yin, F. Huo, *RSC Adv.* **2015**, *5*, 2191–2206; b) J. Chen, Y. Li, K. Lv, W. Zhong, H. Wang, Z. Wu, P. Yi, J. Jiang, *Sens. Actuators B* **2016**, *224*, 298–306; c) X. Han, Y. Ding, J. Yu, K. Li, D. Zhao, B. Chen, *ACS Appl. Mater. Interfaces* **2021**, *13*, 20371–20379.
- [17] a) N. Yoshinari, N. Kuwamura, T. Kojima, T. Konno, *Coord. Chem. Rev.* **2023**, *474*, 214857; b) N. Yoshinari, T. Konno, *Coord. Chem. Rev.* **2023**, *474*, 214850.
- [18] a) M. Ueda, Z. L. Goo, K. Minami, N. Yoshinari, T. Konno, *Angew. Chem. Int. Ed.* **2019**, *58*, 14673–14678; b) Z. L. Goo, K. Minami, N. Yoshinari, T. Konno, *Chem. Asian J.* **2021**, *16*, 2641–2647.
- [19] N. Yoshinari, Z. L. Goo, K. Nomura, T. Konno, *Inorg. Chem.* **2023**, *62*, 9291–9294.
- [20] M. Kouno, K. Minami, N. Kuwamura, T. Konno, *Chem. Lett.* **2019**, *48*, 122–125.
- [21] D. Kim, J. Han, O.-S. Jung, Y.-A. Lee, *RSC Adv.* **2022**, *12*, 25118–25122.
- [22] R. D. Shannon, *Acta Crystallogr.* **1976**, *A32*, 751–767.
- [23] N. V. S. Harisomayajula, S. Makovetskyi, Y.-C. Tsai, *Chem. Eur. J.* **2019**, *25*, 8936–8954.
- [24] In crystal, two of four *fac*- $[\text{Rh}(\text{aet})_3]$ units and five of six Cu^I atoms are disordered over two positions in a 3:1 ratio, which is assigned to the disorder of the same isomer in two positions (Figure S2).
- [25] $[1^{\text{Rh}}]^{4+}$ is the first cationic coordination compound with a $[\text{Cu}_6\text{S}]^{4+}$ core, although two anionic compounds with a $[\text{Cu}_6\text{S}]^{4+}$ core have been reported.^[14,36]
- [26] Attempts to synthesize $[\text{Cu}_3\{\text{Ir}(\text{apt})_3\}_2](\text{BF}_4)_3$ as a pure species were unsuccessful because of its high air-sensitivity, which precluded to investigate the reaction of $[\text{Cu}_3\{\text{Ir}(\text{apt})_3\}_2]^{3+}$ with NaSH.
- [27] A crude sample of $[2^{\text{Rh}}](\text{BF}_4)_2$, which was obtained by the insufficient removal of a precipitate, showed weak powder X-ray diffractions due to Cu_2S , besides major diffractions due to $[2^{\text{Rh}}]^{2+}$ (Figure S10). This implies the removal of Cu^I from $[\text{Cu}_3\{\text{Rh}(\text{apt})_3\}_2]^{3+}$ to form Cu_2S .
- [28] The retention of the structures in $[1^{\text{Rh}}]^{4+}$, $[1^{\text{Ir}}]^{4+}$, and $[2^{\text{Rh}}]^{2+}$ in solution was supported by the ESI-mass spectra (Figures S11–S13).
- [29] a) M. Kouno, N. Kuwamura, N. Yoshinari, T. Konno, *Angew. Chem. Int. Ed.* **2017**, *56*, 13762; b) M. Kouno, N. Kuwamura, N. Yoshinari, T. Konno, *Chem. Lett.* **2017**, *5*, 1542.
- [30] S. Kawaguchi, M. Takemoto, K. Osaka, E. Nishibori, C. Moriyoshi, Y. Kubota, Y. Kuroiwa, K. Sugimoto, *Rev. Sci. Instrum.* **2017**, *88*, 085111.
- [31] Gaussian 09, Revision A.02, M. J. Frisch, G. W. Trucks, H. B. Schlegel, G. E. Scuseria, M. A. Robb, J. R. Cheeseman, G. Scalmani, V. Barone, G. A. Petersson, H. Nakatsuji, X. Li, M. Caricato, A. Marenich, J. Bloino, B. G. Janesko, R. Gomperts, B. Mennucci, H. P. Hratchian, J. V. Ortiz, A. F. Izmaylov, J. L. Sonnenberg, D. Williams-Young, F. Ding, F. Lipparini, F. Egidi, J. Goings, B. Peng, A. Petrone, T. Henderson, R. Ranasinghe, V. G. Zakrzewski, J. Gao, N. Rega, G. Zheng, W. Liang, M. Hada, M. Ehara, K. Toyota, R. Fukuda, J. Hasegawa, M. Ishida, T. Nakajima, Y. Honda, O. Kitao, H. Nakai, T. Vreven, K. Throssell, J. A. Montgomery, Jr., J. E. Peralta, F. Ogliaro, M. Bearpark, J. J. Heyd, E. Brothers, K. N. Kudin, V. N. Staroverov, T. Keith, R. Kobayashi, J. Normand, K. Raghavachari, A. Rendell, J. C. Burant, S. S. Iyengar, J. Tomasi, M. Cossi, J. M. Millam, M. Klene, C. Adamo, R. Cammi, J. W. Ochterski, R. L. Martin, K. Morokuma, O. Farkas, J. B. Foresman, and D. J. Fox, Gaussian, Inc., Wallingford CT, 2016.

- [32] G. N. Sheldrick, *Acta Crystallogr. Sect. C* **2015**, A71, 3–8.
- [33] O. V. Dolomanov, L. J. Bourhis, R. J. Gildea, J. A. K. Howard, H. J. Puschmann, *J. Appl. Crystallogr.* **2009**, 42, 339–341.
- [34] Deposition numbers 2336996 (for $[\text{Cu}_3\{\text{Ir}(\text{aet})_3\}_2](\text{BF}_4)_3 \cdot \text{CH}_3\text{CN}$), 2320487 (for $[\text{1}^{\text{Rh}}](\text{BF}_4)_2(\text{SiF}_6)$), 2320486 (for $[\text{1}^{\text{Ir}}](\text{BF}_4)_4$), and 2320485 (for $[\text{2}^{\text{Rh}}](\text{BF}_4)_2 \cdot 2\text{MeOH}$) contain the supplementary crystallographic data for this paper. These data are provided free of charge by the joint Cambridge Crystallographic Data Centre and Fachinformationszentrum Karlsruhe Access Structures service.
- [35] T. Konno, K. Nakamura, K. Okamoto, J. Hidaka, *Bull. Chem. Soc. Jpn.* **1993**, 66, 2582–2589.
- [36] P. Lin, X.-T. Wu, L. Chen, L.-M. Wu, W.-X. Du, *Polyhedron* **2000**, 19, 2189–2193.

Manuscript received: March 8, 2024
 Revised manuscript received: April 23, 2024
 Accepted manuscript online: April 28, 2024
 Version of record online: ■ ■, ■ ■

RESEARCH ARTICLE

The $\{\text{Cu}^{\text{I}}_3\}^{3+}$ moiety supported by two octahedral metalloligands with 5-membered vs. 6-membered N,S-chelate rings is converted to $\{\text{Cu}^{\text{I}}_6\text{S}\}^{4+}$ vs. $\{\text{Cu}^{\text{I}}_2\}^{2+}$ by reacting with S^{2-} , showing that the sulfide-induced structural expansion vs. contraction is regulated by the small difference in the chelated ring sizes.



Dr. Z. L. Goo, Dr. N. Yoshinari*, Y. Yasukawa, K. Minami, Prof. T. Konno*

1 – 8

Sulfide-Induced Dimerization Versus Demetallation of Tricopper(II) Clusters Protected by Tris-Thiolato Metalloligands

